

# Propofol Breath Monitoring as a Potential Tool to Improve the Prediction of Intraoperative Plasma Concentrations

Pieter Colin<sup>1,2</sup> · Douglas J. Eleveld<sup>1</sup> · Johannes P. van den Berg<sup>1</sup> · Hugo E. M. Vereecke<sup>1</sup> · Michel M. R. F. Struys<sup>1,3</sup> · Gustav Schelling<sup>5</sup> · Christian C. Apfel<sup>4</sup> · Cyrill Hornuss<sup>5</sup>

Published online: 29 December 2015  
© Springer International Publishing Switzerland 2015

## Abstract

**Introduction** Monitoring of drug concentrations in breathing gas is routinely being used to individualize drug dosing for the inhalation anesthetics. For intravenous anesthetics however, no decisive evidence in favor of breath concentration monitoring has been presented up until now. At the same time, questions remain with respect to the performance of currently used plasma pharmacokinetic models implemented in target-controlled infusion systems. In this study, we investigate whether breath monitoring of propofol could improve the predictive performance of currently applied, target-controlled infusion models.

**Methods** Based on data from a healthy volunteer study, we developed an addition to the current state-of-the-art pharmacokinetic model for propofol, to accommodate breath concentration measurements. The potential of using this pharmacokinetic (PK) model in a Bayesian forecasting setting was studied using a simulation study. Finally, by

introducing bispectral index monitor (BIS) measurements and the accompanying BIS models into our PK model, we investigated the relationship between BIS and predicted breath concentrations.

**Results and Discussion** We show that the current state-of-the-art pharmacokinetic model is easily extended to reliably describe propofol kinetics in exhaled breath. Furthermore, we show that the predictive performance of the a priori model is improved by Bayesian adaptation based on the measured breath concentrations, thereby allowing further treatment individualization and a more stringent control on the targeted plasma concentrations during general anesthesia. Finally, we demonstrated concordance between currently advocated BIS models, relying on predicted effect-site concentrations, and our new approach in which BIS measurements are derived from predicted breath concentrations.

## Key Points

On-line measurements of exhaled propofol concentrations improve the predictive performance of the current state-of-the-art pharmacokinetic model.

Individually predicted exhaled propofol concentrations provide an easy target to individualize anesthetic dosing regimens.

✉ Pieter Colin  
P.J.Colin@umcg.nl

<sup>1</sup> Department of Anesthesiology, University Medical Center Groningen, University of Groningen, Hanzeplein 1, Postbus 30 001, Groningen 9700 RB, The Netherlands

<sup>2</sup> Laboratory of Medical Biochemistry and Clinical Analysis, Faculty of Pharmaceutical Sciences, Ghent University, Ghent, Belgium

<sup>3</sup> Department of Anesthesia, Ghent University, Ghent, Belgium

<sup>4</sup> Department of Epidemiology and Biostatistics, University of California, San Francisco, CA, USA

<sup>5</sup> Department of Anaesthesiology, Klinikum der Universität München, Munich, Germany

## 1 Introduction

In anesthesiology, pharmacokinetic (PK) modeling is used extensively to develop target-controlled infusion (TCI) systems. These systems use an established population PK

model to estimate the required dosing regimen to be given to an individual patient to achieve and maintain a predefined target plasma (or effect-site) concentration. Although its use is becoming standard of care for the administration of intravenous anesthetics such as propofol, concerns remain with respect to the accuracy of these systems.

Monitoring of drug concentrations in combination with a Bayesian adaptation of the a priori model could potentially address these concerns. Motamed et al. [1] and Maitre et al. [2] showed in a retrospective study that for rocuronium and alfentanil, respectively, Bayesian forecasting, based on timely plasma measurements, could improve the predictive performance of intraoperative plasma concentrations.

For propofol, clinical trials evaluating the predictive performance of currently used TCI models are ongoing [3, 4]. In addition to identifying the shortcomings of currently implemented propofol PK models (i.e., Marsh [5], Schnider [6], and/or Eleved [7]), these studies could distinguish whether a Bayesian forecasting based on intermittent plasma sampling using conventional [3] or bedside measurement systems [4] could improve the predictive performance of current TCI systems. Recently, as step-up to these iterative blood sampling strategies, several groups focused on developing a measurement system that could detect propofol in exhaled breathing gas in real time.

Although not conventionally applied to intravenous anesthetics, monitoring of drug concentrations in breathing gas is not new. Moreover, it is routinely being used to individualize drug dosing for the inhalation anesthetics (isoflurane and sevoflurane) [8, 9]. One of the advantages of following up on the exhaled drug concentration is that in this way the arterial concentration, which is proportional to the alveolar concentration, is controlled throughout the anesthetic procedure.

Unlike other intravenous anesthetics, propofol has a very high vapor pressure ( $3.1 \times 10^{-3}$  mmHg at 25 °C). Fentanyl, for example, another intravenous agent, has a 100,000-fold lower vapor pressure ( $5.5 \times 10^{-8}$  mmHg at 25 °C). This physicochemical property allows propofol to readily distribute from the arterial (capillary) blood into the alveolar gas, thereby facilitating its possible detection in breathing gas.

At the moment, research is ongoing to develop the necessary detection systems as well as the accompanying control systems/PK models necessary to implement online breath analysis for propofol. Several groups [10–14], using a variety of detection systems from ion mobility spectrometry (IMS) and ion molecule reaction mass spectrometry (IMR-MS) to electrochemical sensors, showed that it is possible to detect propofol in breathing gas during clinically relevant dosing regimens.

To date, to the best of our knowledge, three groups explored the possibility of applying compartmental modeling to describe propofol breath kinetics. Kreuer et al. [14] and Ziaian et al. [10] described propofol breath kinetics in human volunteers ( $n = 1$  and 17, respectively) using a compartmental pharmacokinetic model and a ‘PT1 model’, respectively. The latter is also known as a ‘low-pass filter’ and is frequently used in acoustics engineering. Varadarajan et al. [11] used a compartmental modeling approach to describe propofol breath kinetics in pigs. In these studies, propofol breath concentrations were measured using IMR-MS [11], IMS [14], and an electrochemical sensor [10], respectively.

To integrate the breath concentration measurements with the plasma PK of propofol, two of these authors (Varadarajan et al. [11] and Kreuer et al. [14]) used predicted propofol plasma concentrations (Marsh model [5]), whereas Ziaian et al. [10] used post hoc estimates of the Marsh model [5], tailored to measure propofol plasma concentrations, to serve as inputs for their breath models. None of the papers explored population PK modeling as a tool to simultaneously describe propofol plasma and breath kinetics, nor did these authors investigate the potential clinical utility of monitoring propofol breath concentrations to predict plasma PK.

Therefore, using data from a healthy volunteer study, we set out to (i) develop an extension, to the current state-of-the-art propofol plasma PK model, capable of describing the exhalation kinetics of propofol and (ii) evaluate Bayesian forecasting based on measured propofol breath concentrations as a potential tool to improve the predictive performance of intraoperative propofol plasma concentrations. Furthermore, the usefulness of predicted breath concentrations as a predictor for the cerebral effects of propofol, as measured by the bispectral index monitor (BIS), was explored by comparing against frequently used BIS models.

## 2 Methods

### 2.1 Study Design

The study was approved by the institutional review board and was carried out in concordance with the International Conference on Harmonisation Guidelines for Good Clinical Practice (NCT01191021). After written informed consent, 20 healthy volunteers (American Society of Anesthesiologists status I, age >18 years) underwent general anesthesia with propofol (Diprivan® 1%, London, UK). The volunteers received  $0.4 \text{ mg kg}^{-1} \text{ min}^{-1}$  propofol via a venous catheter for 10 min followed by a 20-min recovery period. Afterwards, administration was resumed

using a TCI, based on Schnider et al. [6]. The TCI protocol consisted of four target plasma concentrations (2, 3, 4, and 5  $\mu\text{g mL}^{-1}$ ), which were maintained for 15 min each. Ninety minutes after the start of the experiment the infusion was stopped and the study subjects were left to recover from anesthesia.

## 2.2 Propofol Measurements in Plasma ( $C_{\text{plasma}}$ )

Arterial blood samples were centrifuged immediately after drawing. Blood plasma was then separated and frozen at  $-20\text{ }^{\circ}\text{C}$  temperature. The plasma samples were analyzed within 8 weeks after the experiments using an in-house-developed method. Propofol plasma concentrations were determined with a liquid-chromatography tandem mass spectrometry assay. The lower limit of detection and quantification of the method were 60 and 100  $\text{ng mL}^{-1}$ , respectively.

## 2.3 Propofol Breath Measurements ( $C_{\text{breath}}$ )

Breathing gas was sampled at 50 mL/min through a T-piece attached to the laryngeal mask of the study participants. An IMR-MS (V&F Medical Development GmbH, Absam, Austria) [15] was used to measure propofol in the sampled gas within 500 ms. To distinguish between inspiratory and expiratory air, a second mass spectrometry system based on electron impact-determined carbon dioxide concentrations 10 times/s was used. Expiratory propofol data were extracted as the median expiratory breath signal of 30-s intervals from the recorded breath data as described previously [15].

## 2.4 Determination of Propofol Cerebral Drug Effect (BIS)

The effect of propofol on the brain was determined with the BIS (BIS Vista system, Covidien, Boulder, CO, USA). The BIS transforms the electroencephalogram into a dimensionless index ranging from 100 (fully awake individual) to 0 (deep anesthesia with isoelectric EEG activity). BIS smoothing time was set to 10 s and BIS values were recorded every second.

## 2.5 Available Data

The final dataset included a median of 22 (range 19–23) arterial plasma propofol concentrations, 208 (range 118–272) propofol breath concentrations, and 300 (range 220–379) BIS measurements per subject. An overview of the characteristics of the healthy volunteers in our study is given in Table 1.

**Table 1** Characteristics of the study population. All included patients had American Society of Anesthesiologists status I

Characteristic	Mean (range)
Age (years)	27 (22.8–33.3)
Weight (kg)	74.1 (63.8–83.0)
Height (cm)	168.0 (162.2–178.5)
Sex ( <i>n</i> , male/female)	9/11

To reduce the computational burden during model development, we reduced the number of propofol breath and BIS measurements per subject. At the same time, we applied a median filter (span equal to 5 s) to reduce the influence of outlying data during model development. In summary: the first out of every 10 consecutive median-filtered datapoints were retained in the dataset, resulting in a median of 22 and 30 measurements for the breath and BIS data, respectively.

For the prospective evaluation of the applicability of the Bayesian forecasting approach, all of the available breath concentration measurements were used.

## 2.6 Model Building of the PK Model to Describe Propofol Breath Kinetics

We used the first-order conditional estimation algorithm with interaction as implemented in NONMEM<sup>®</sup> (version 7.3; Icon Development Solutions, Hanover, MD, USA) to fit different breath models to our dataset. As a starting point for our model building, we used the individual PK parameters (IPP) approach [16]. For this approach, individual post-hoc PK parameters ( $CL$ ,  $Q_2$ ,  $Q_3$ ,  $V_1$ ,  $V_2$ , and  $V_3$ ) were derived from the Eleveld [7] model and were fixed for each individual during the subsequent evaluation of different breath models.

Our choice for the Eleveld model as an a priori model, rather than developing a PK model specific for this study population or using another published propofol PK model, was based on the model's documented general applicability and superior predictive performance in a wide variety of patient populations [7], making it, at the moment, state of the art.

Model building started with a structural model similar to the model proposed by Ziaian et al. [10]. This model was implemented using an effect compartment ( $ke0_{\text{Lung}}$ ) and a scale parameter ( $K$ ). The former was used to correct for the reported hysteresis between propofol plasma and breath concentrations, whereas the latter was used to accommodate a.o., the unit conversion from  $\mu\text{g/mL}$  for the plasma measurements to parts per billion (ppb) for the measured breath concentrations.

Different modifications to this structural model were compared using the Akaike Information Criterion (AIC). Furthermore, as a safeguard to over-parameterization, cross-validation was performed to compare the goodness-of-fit (GOF) of the different breath models. Once population parameter estimates were obtained by fitting the breath models to the training cohort, the GOF of the post-hoc estimates of these model were evaluated in the validation cohorts. This process was repeated four-fold, each time allocating  $\frac{1}{4}$  and  $\frac{3}{4}$  of the dataset to the validation and training cohort, respectively. Care was taken such that each subject in the dataset was allocated to a validation cohort once.

GOF, in terms of propofol breath concentrations in the validation cohort, was evaluated graphically in R<sup>®</sup> (R Foundation for Statistical Computing, Vienna, Austria) and numerically using the median prediction error (MdPE) and the root mean square error (RMSE).

## 2.7 Application of Bayesian Forecasting to Predict Intraoperative Propofol Plasma Concentrations

To evaluate the clinical utility of the final model (i.e., the potential to improve the predictive performance of the a priori model), we conducted a simulation study. In this study, similar to the cross-validation described earlier, the final model was first fit to the training set. At this stage, the population PK parameters & data approach [16], which is known to produce less biased parameter estimates as compared with the IPP approach (at the expense of computing time), was used. In other words, during the estimation process the population parameters from the Eleveld model were fixed whilst allowing the parameters from the breath model to be estimated.

Next, using the parameter estimates for the breath model from the training set, the predictive performance was evaluated in a validation cohort in which the  $C_{\text{plasma}}$  were removed (i.e., the model was blinded for the measured propofol plasma concentrations to mimic the clinical situation where these concentrations are generally unknown). To study the change in predictive performance over time, this process was repeated for several datasets, differing from each other in the number of breath measurements that were used to predict propofol plasma concentrations (32 datasets in total, containing 1 min up until 100 min of breath concentration measurements). Predictive performance, during the propofol infusion regimens (i.e., the intraoperative timeframe), summarized in terms of MdPE and RMSE, was calculated by contrasting  $C_{\text{plasma}}$  with the predicted propofol concentrations.

## 2.8 PKPD Model for the Cerebral Effects of Propofol

As a final evaluation towards the usefulness of continuous monitoring of propofol breath concentrations, we explored

to what extent these breath concentrations could be used to explain/predict the cerebral effects of propofol. To this end, as a reference PKPD model, a simplified version of the model proposed by Bjornsson et al. [17] was added to our final model. The simplification consisted of using a single-rather than a double-effect compartment to model the hysteresis between  $C_{\text{plasma}}$  and BIS measurements. In line with the model proposed by Bjornsson et al., the predicted effect side concentration ( $C_e$ ) was used as a predictor in a sigmoid  $E_{\text{max}}$  model to describe changes in BIS (Eq. 1):

$$\text{BIS} = \text{BL}_{\text{BIS}} - E_{\text{max}} \times \frac{C_e^\gamma}{EC_{50}^\gamma + C_e^\gamma} \quad (1)$$

To evaluate the correlation between the individually predicted breath concentrations ( $\text{IPRED}_{\text{breath}}$ ) and the BIS measurements, we fitted an additional model in which the  $\text{IPRED}_{\text{breath}}$  from our final model were used in the sigmoid  $E_{\text{max}}$  model (Eq. 1) instead of the  $C_e$  (this model required 1 parameter less, i.e., the  $\text{ke0}_{\text{BIS}}$  associated with the  $C_e$ ).

## 3 Results

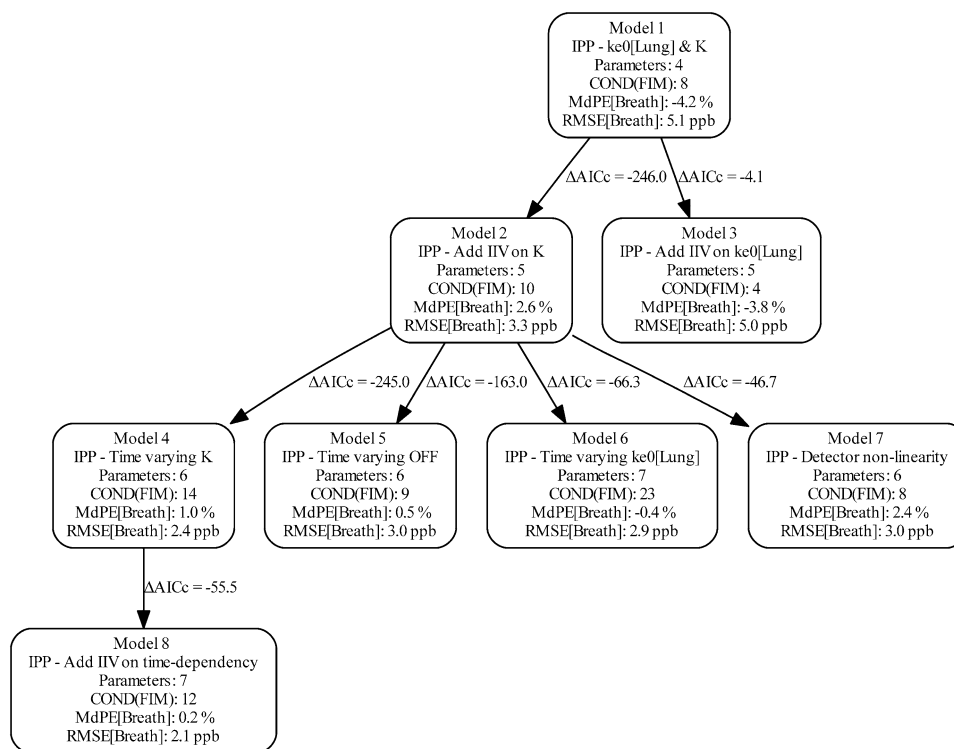
### 3.1 Model Building

As a starting point, we decided to model propofol breath kinetics using a structural model similar to the model proposed by Ziaian et al. [10]. Subsequently, several modifications to this structural model were explored (Fig. 1). Addition of a parameter describing inter-individual-variability (IIV) on  $K$  significantly improved the model's GOF ( $\Delta\text{AIC}$ :  $-246.0$ ).

Furthermore, to correct for a significant time-varying bias in the residual plots, four different modifications were explored. Model 4 assumed that  $K$  changes over time, an effect that could be expected from propofol effects on the ventilation-perfusion status of a patient. Initially, we implemented this using an indirect response model, linking the propofol blood concentrations to the stimulation/inhibition of a latent variable which, in turn, drives a change in  $K$  (an approach similar to the latent variable approach in Troconiz et al. [18]). Nevertheless, based on the data, this was reduced to a simple linear time-dependent change in  $K$  over time.

Model 5 explored the possibility of a baseline drift in the measurement system owing to for example, a gradual built-up of propofol, a compound that is known to have a high affinity for plastics because of its high lipophilicity [19]. Model 6 explored the possibility of a time-varying  $\text{ke0}_{\text{Lung}}$ . This is in line with Bjornsson et al. [17], who showed that propofol plasma kinetics were time dependent. Finally, model 7 evaluated whether a non-linear detector response could be at the origin of this time-dependent bias in the residuals.

**Fig. 1** Model building hierarchy



All four tested models significantly improved the model's GOF, leading to a decrease in AIC of 245.0, 163.0, 66.3, and 46.7, respectively. However, as shown in Fig. 2, only model 4 successfully removed the residual bias across the entire observation period. Finally, to model 4, another random-effect parameter was added to allow IIV on the time dependency of K (denoted by a 'slope' parameter), thereby further lowering the MdPE and RMSE to 0.2 % and 2.1 ppb, respectively. The GOF for the final model (i.e., model 8 in Fig. 1) is shown in Fig. 3, parameter estimates are given in Table 2.

### 3.2 Application of Bayesian Forecasting to Predict Intraoperative Propofol Plasma Concentrations

Figure 4 shows the  $C_{\text{plasma}}$  (for which the model was blinded) and the first 30 min of measured propofol breath concentrations for a representative individual from our study. From this figure, it stands out that for this individual the predicted plasma concentrations from the a priori model (solid line) are somewhat biased, thereby underestimating the  $C_{\text{plasma}}$ . After 30 min, we used the measured  $C_{\text{breath}}$  up until that point to produce the post hoc predictions from our final model (dashed lines). When comparing the predicted plasma concentrations against the  $C_{\text{plasma}}$  for both approaches, it stands out that, for this individual, the post hoc predicted plasma concentrations from our final model are in closer resemblance to the  $C_{\text{plasma}}$  than the a

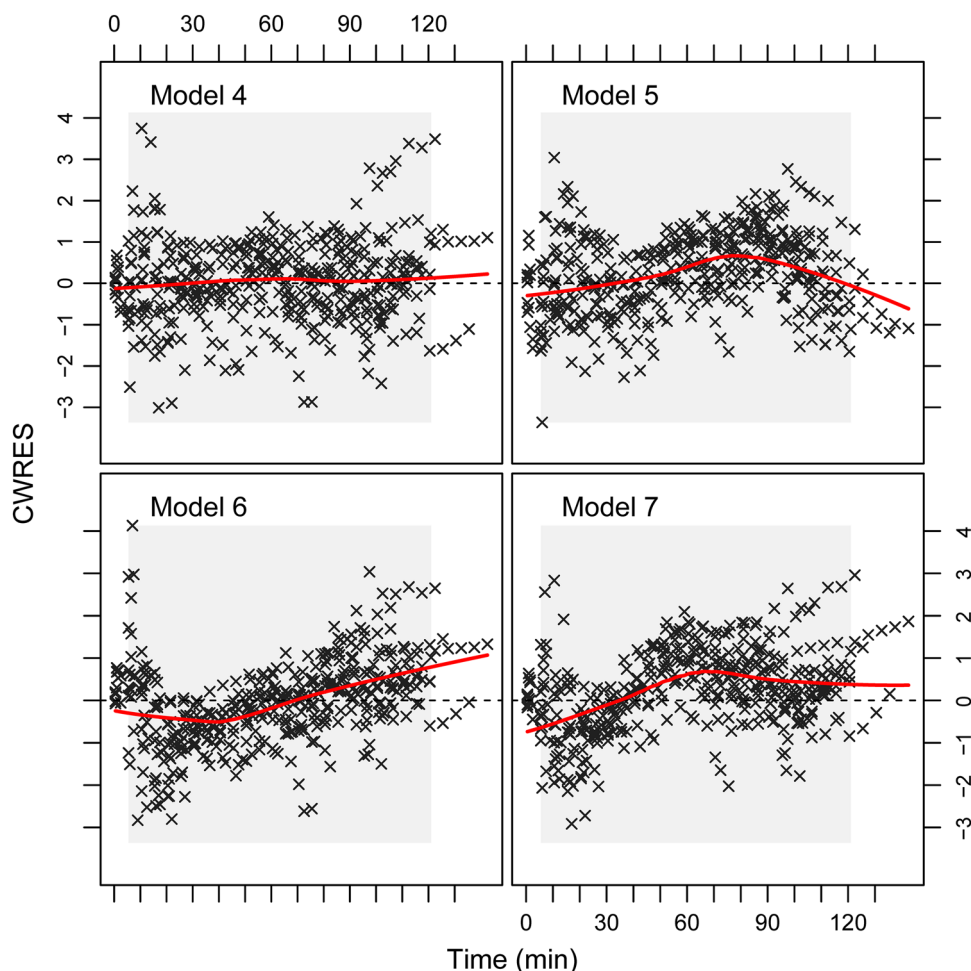
priori predictions, thereby emphasizing the validity of our proposed approach.

Next, to fully explore the potential of this approach, this process was repeated using different time-frames of breath concentrations to predict the intraoperative propofol plasma concentrations, i.e., concentrations up until the last propofol infusion was stopped. Figure 5 shows the change in predictive performance when including increasing amounts of breath concentrations.

From this figure, it is seen that the overall MdPE in the study population (red line in Fig. 5) decreases from 42.8 %, when no breath concentrations are used (i.e., the a priori MdPE), to an MdPE of  $-1.05$  % when more than 35 min of breath concentrations are used. This indicates that, on a population level, our approach succeeds in reducing the apparent bias that is present in the a priori model. On an individual level, for 11/20 of the volunteers in our study, the initial bias is reduced (mean reduction 31.5 %, range 1.3–78.4 %) and for the nine subjects the bias slightly increases (mean increase 11.8 %, range 2.9–31.0).

When looking at the RMSE (bottom panel of Fig. 5), a performance metric related to the precision of the predictions, we see that on a population level it reduces from 1.63  $\mu\text{g/mL}$ , for the a priori predictions, to 1.39  $\mu\text{g/mL}$ , when using the full time course of the  $C_{\text{breath}}$  to predict the intraoperative propofol plasma concentrations. On an individual level, the subjects whose bias was reduced

**Fig. 2** A plot of the conditionally weighted residuals (CWRES) vs time for the different models evaluated to correct for the observed time-dependent model misspecification. Only model 4, which consists of a linearly increasing  $K$  over time, is able to completely reduce the residual time-dependent bias



benefit from an average decrease in RMSE of  $0.8 \mu\text{g/mL}$  (range  $0.1\text{--}1.3$ ), whereas the other nine subjects show an average increase in RMSE of  $0.6 \mu\text{g/mL}$  (range  $0.1\text{--}2.3$ ).

### 3.3 Predicted Breath Concentrations vs $C_e$ as a Predictor for Propofol Cerebral Drug Effects

To study whether  $\text{IPRED}_{\text{breath}}$  could be a useful surrogate to the traditional predicted propofol effect-site concentrations ( $C_e$ ), as implemented in the model proposed by Bjornsson et al. [17], we compared two different PKPD models for the BIS measurements (a graphical presentation of both models is given in Fig. 6).

As seen from Table 2, judging from the similar residual error standard deviations ( $0.47$  and  $0.45$  for  $C_e$  and  $\text{IPRED}_{\text{breath}}$  model, respectively), both models describe the change in BIS measurements to a similar degree. Furthermore, from the concordance between all other estimated parameters (except for  $\text{EC}_{50}$ , which has different dimensions in both models) and the similarity in AIC ( $4401$  and  $4379$ , for  $C_e$  and  $\text{IPRED}_{\text{breath}}$  model, respectively), it seems

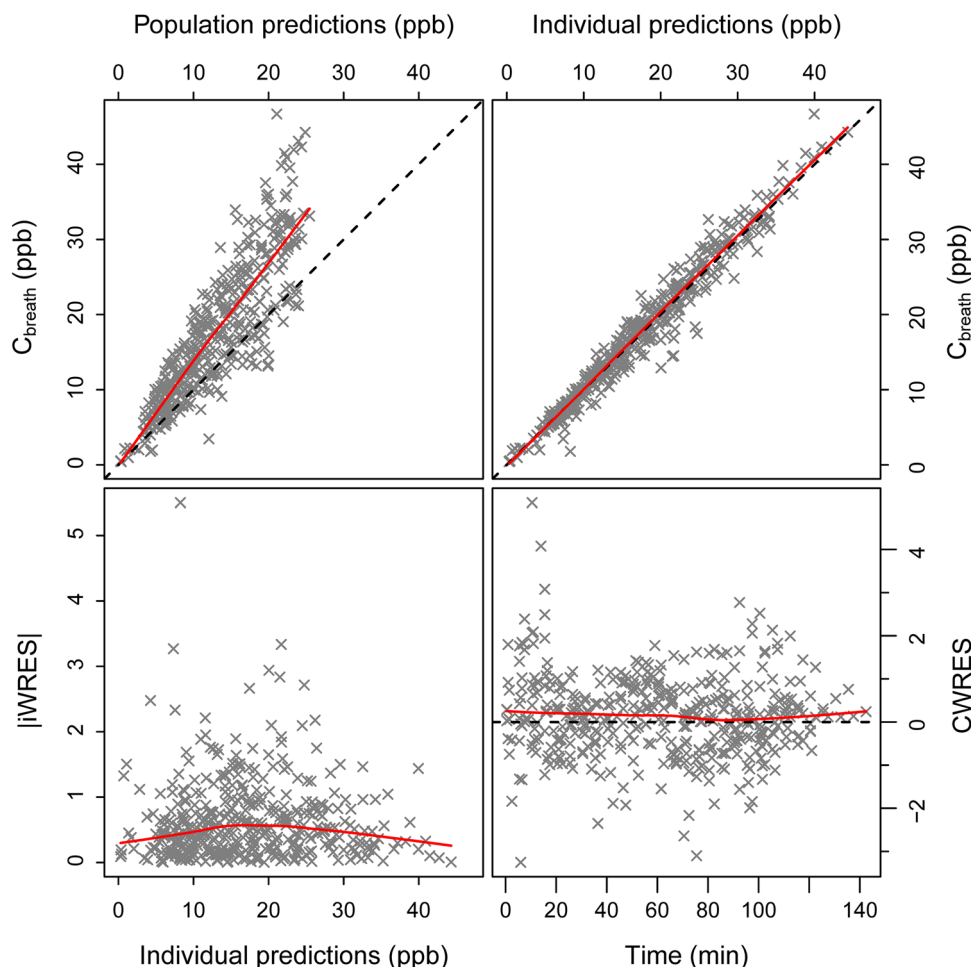
that both the  $C_e$  and  $\text{IPRED}_{\text{breath}}$  from our final model could be used interchangeably to predict/describe the effects of propofol on the BIS index.

## 4 Discussion

Using data from a healthy volunteer study, we set out to develop an extension, to the current state-of-the-art propofol plasma PK model [7], capable of describing the exhalation kinetics of propofol. The final parameter estimates for  $\text{ke}_{0\text{Lung}}$  and  $K$  ( $0.152 \text{ min}^{-1}$  and  $3.56 \text{ ppb mL } \mu\text{g}^{-1}$ , respectively), describing the hysteresis and the proportional difference between  $C_{\text{plasma}}$  and  $C_{\text{breath}}$ , are very similar to the work of Ziaian et al. [10] who reported a median  $\text{ke}_{0\text{Lung}}$  (in the paper referred to as  $k_{L10}$ ) of  $0.155 \text{ min}^{-1}$  and median  $K$  of  $2.71 \text{ ppb mL } \mu\text{g}^{-1}$ .

Although the clinical conditions (i.e., the propofol infusion regimen) were fairly similar in their study, it inspires confidence that Ziaian et al. [10] reported similar parameter estimates based on the detection of propofol breath concentrations using a chemical sensor rather than

**Fig. 3** Goodness-of-fit plot of the final model (model 8). Parameter estimates, obtained using the individual pharmacokinetic parameters approach, as described in the Sect. 2, are given in Table 2. The *top-left panel* shows the apparent bias in the a priori model, which is passed on to the population predictions for the breath concentrations ( $C_{\text{Breath}}$ ) of the final model. The *bottom panels* show the absolute individually weighted residuals (iWRES) vs individual predictions and the conditionally weighted residuals (CWRES) vs time



IMR-MS. On the contrary, Kreuer et al. [14] reported different parameter estimates. Although their estimated  $ke_{0_{\text{Lung}}}$  (referred to as  $k_{1L}$  in the publication) is slightly similar to ours ( $0.209 \text{ min}^{-1}$ ), their estimate for  $K$  is very different ( $K$  was calculated from their publication as  $k_{L1}/k_{1L}$  and was  $0.66 \text{ ppb mL } \mu\text{g}^{-1}$ ). The latter difference is in line with the differences in measured propofol breath concentrations between their study (maximum in between 0.6 and 0.8 ppb) and ours (maximum equals 53 ppb). Although we cannot provide a clear explanation for this discrepancy, it seems that causes other than the propofol dosing regimen (at their  $3 \mu\text{g/mL}$  TCI target, propofol breath concentrations are  $>10$  ppb in our study), such as intrinsic issues with the IMS detection system, the systems used for calibration, or the fact that they only studied a single subject rather than a population, might explain the difference in the parameter estimates.

An important part of our model building was devoted to the exploration of potential mechanisms that could give rise to a time-dependent model misspecification. Models 5 and 7 showed that correcting for intrinsic detector-related issues, such as drift (model 5) and detector non-linearity,

were not sufficient to remove the apparent bias. Furthermore, a correction for the potential time-dependent kinetics of propofol, an approach earlier proposed by Bjornsson et al. [17], only slightly improved the model's GOF without completely reducing the model misspecification. Model 4, which incorporates a linearly increasing  $K$  over time, was the only model that could completely remove the observed time-dependent bias in the residual plots.

In our opinion, there are several possible mechanisms that could explain this time dependency. First, an instrument-related issue causing the sensitivity of the detector to increase over time, might explain this phenomenon. Second, the time-dependent bias might originate from the propagation of a model misspecification in the plasma PK part of the model, i.e., the Eleveld model. Indeed, when we look at the conditionally weighted residuals for the Eleveld post-hoc plasma concentration predictions for our subjects, a qualitatively similar pattern is observed (figure not shown). However, when we fit a custom three-compartmental PK model combined with our proposed breath model to the data, the CWRES plot for the plasma

**Table 2** Final parameter estimates and associated standard errors for our final model (model 8), which was obtained using an individual pharmacokinetic parameters approach (IPP) approach where breath concentrations were modeled, keeping the plasma pharmacokinetic parameters fixed to the post-hoc estimates of the a priori model.

Furthermore, parameter estimates are shown for two models evaluating the cerebral effects of propofol as a function of a modeled plasma effect-side concentration ( $C_e$ ) and predicted breath concentrations (IPRED<sub>breath</sub>), respectively

Parameter	Model 8		BIS-f( $C_e$ )		BIS-f(IPRED <sub>breath</sub> )	
	$C_{\text{plasma}}$ (IPP) and $C_{\text{breath}}$		$C_{\text{plasma}}$ (IPP) and $C_{\text{breath}}$ & BIS		$C_{\text{plasma}}$ (IPP) and $C_{\text{breath}}$ & BIS	
	Estimate	RSE (%)	Estimate	RSE (%)	Estimate	RSE (%)
$ke0_{\text{Lung}}$ ( $\text{min}^{-1}$ )	0.152	5.7	0.152	5.7	0.146	9.0
$ke0_{\text{BIS}}$ ( $\text{min}^{-1}$ )			0.107	12.3		
$K$ (ppb mL $\mu\text{g}^{-1}$ )	3.56	6.7	3.56	6.7	3.81	9.0
Slope [ppb mL ( $\mu\text{g min}^{-1}$ )]	0.022	8.8	0.022	8.8	0.017	20.7
$BL_{\text{BIS}}$			94.3	1.0	95.0	1.0
$E_{\text{max}}$			80.9	7.3	77.6	5.6
$EC_{50}$			2.71 $\mu\text{g/mL}$	11.0	12.4 ppb	8.2
$\gamma$			2.43	20.0	2.49	18.6
IIV <sub>K</sub> (%) <sup>a</sup>	23.7	37.6	23.7	37.6	25.8	37.4
IIV <sub>Slope</sub> (%) <sup>a</sup>	40.9	38.2	40.9	38.2	50.8	50.0
IIV <sub><math>E_0</math></sub> <sup>d</sup>			0.716	30.0	0.656	29.1
IIV <sub><math>EC_{50}</math></sub> (%) <sup>a</sup>			28.7	37.1	25.9	42.5
$\sigma_{\text{Plasma}}$ , proportional (%) <sup>c</sup>	21.6		21.6		21.6	
$\sigma_{\text{Breath}}$ , proportional (%) <sup>c</sup>	11.7		11.7		10.3	
$\sigma_{\text{Breath}}$ , additive (ppb) <sup>b</sup>	0.982		0.982		1.40	
$\sigma_{\text{BIS}}$ , additive <sup>b</sup>			0.47		0.45	

$ke0_{\text{Lung}}$  rate constant for the lung effect compartment,  $ke0_{\text{BIS}}$  rate constant for the BIS effect compartment,  $K$  scaling parameter for the lung compartment,  $Slope$  time dependency on  $K$ ,  $BL_{\text{BIS}}$  typical value for the BIS at baseline,  $IIV$  inter-individual variability,  $IIV_{E_0}$  inter-individual variability in baseline BIS,  $\sigma$  standard deviation of residual unexplained variability,  $RSE$  relative standard error,  $BIS$  bispectral index monitor

<sup>a</sup> CV(%) is calculated according to:  $\sqrt{e^{\omega} - 1} \times 100$  %

<sup>b</sup> Residual unexplained variability expressed as a standard deviation

<sup>c</sup> Residual unexplained variability expressed as a relative standard deviation

<sup>d</sup> IIV expressed as a variance in logit domain

concentrations normalize but the time-dependent bias for the breath concentrations remains.

Finally, complex underlying physiological phenomena, such as e.g., venous-arterial mixing, which have been hypothesized in the past to play a role during the first few minutes of propofol dosing [20, 21] and which are currently not addressed in our compartmental PK models might cause this time dependency. Physiologically based PK models, which have been used extensively in the past to describe exhalation kinetics of environmental pollutants [22, 23] or organic solvents [24, 25] and have been applied in the context of propofol PK [26–28], might address these hurdles in the future. Although these models provide superior insights into the physiology behind pharmacokinetic processes in comparison to compartmental PK models, their level of complexity often hinders the clinical implementation.

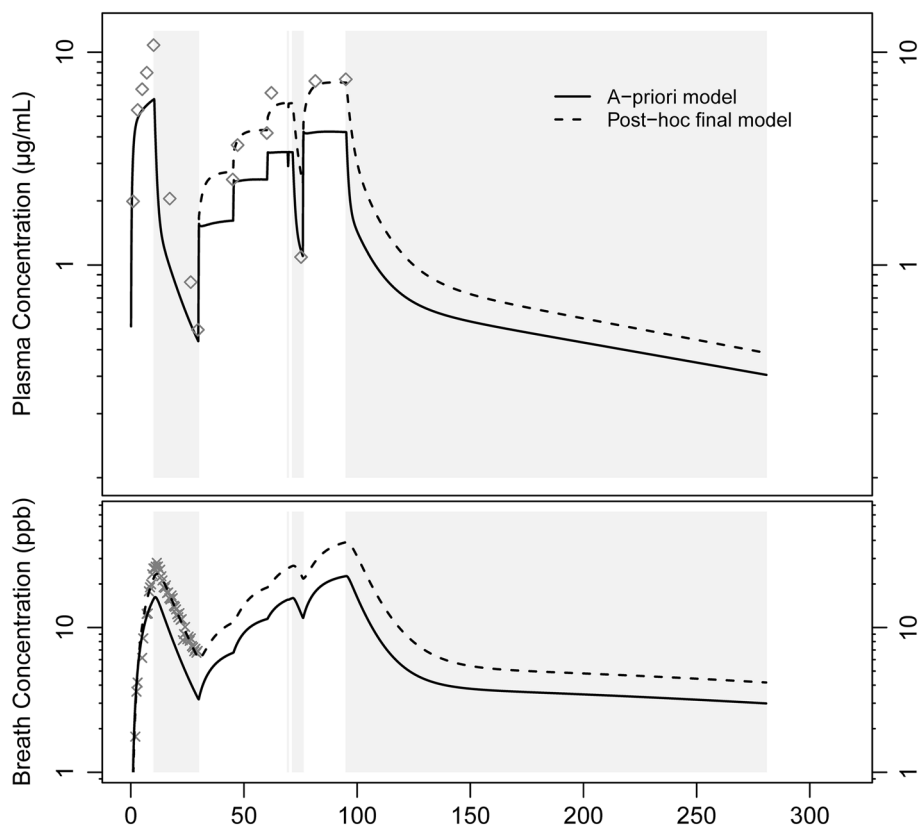
One of our objectives was to evaluate whether a Bayesian forecasting based on measured propofol breath

concentrations could improve the predictive performance of intraoperative plasma concentrations. Figures 4 and 5 clearly show that our proposed approach outperforms the most recent state-of-the-art model available for propofol. Although not all subjects benefit equally from our proposed approach, we showed that the magnitude of the improvements in MdPE and RMSE in the subjects who improved quantitatively outweigh the negative corrections for those who do not benefit from this approach. Overall, on a population level, the bias (MdPE decreased from 42.8 to –1.05 %) as well as the prediction error (RMSE decreased from 1.63 to 1.39  $\mu\text{g/mL}$ , i.e., a 15 % reduction) decreased significantly, demonstrating the clinical usefulness of our proposed approach.

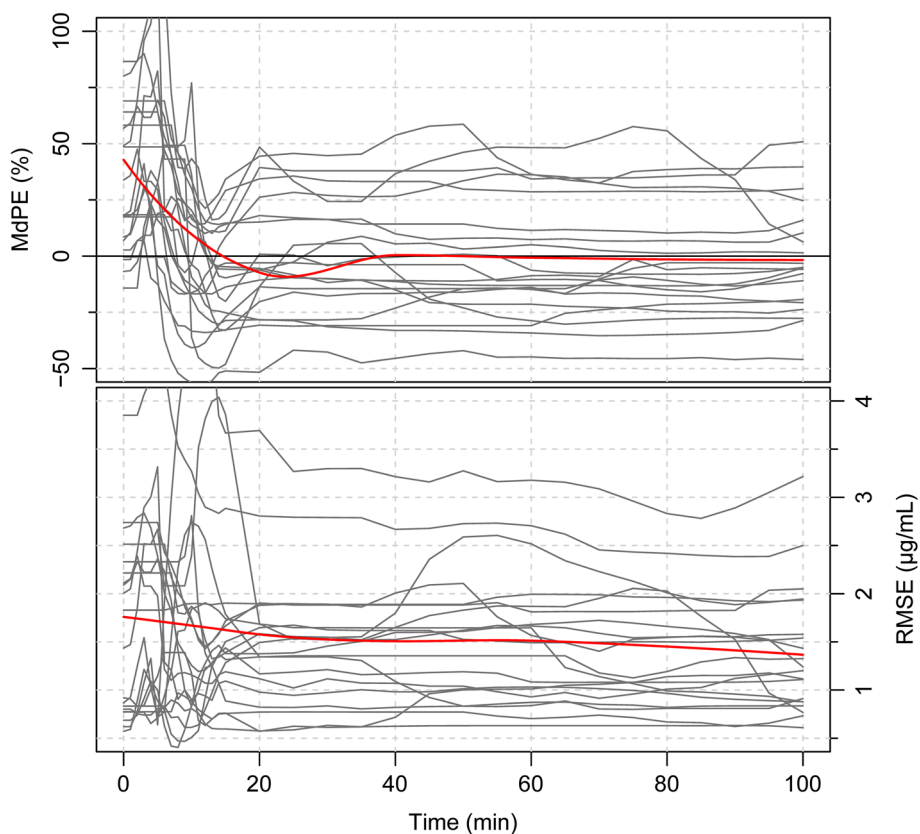
Judging from Fig. 5, no significant improvements are attained beyond 30 min. This effect is most likely explained by the propofol dosing regimen used throughout this study. The initial fast infusion, resulting in a



**Fig. 4** Individual plot of a representative individual showing the measured plasma concentrations ( $C_{\text{plasma}}$ ) [gray diamonds] and model predictions for the a priori model (solid line) and the post-hoc prediction of our final model (dashed line). The Bayesian adaptation of the a priori model was implemented 30 min into the treatment, using the first 30 min of breath concentration measurements only. Of note, during this process the model was blinded for the  $C_{\text{plasma}}$ . To give the reader an impression of the dosing regimen used throughout this study, we used gray-shaded areas to show periods when no drug was infused



**Fig. 5** The change in predictive performance of our proposed approach as a function of the time frame in which breath concentrations are monitored (as indicated in the x-axis). The median prediction error (MdPE) and root mean square error (RMSE) for the different individuals in our study are shown with a gray solid line. The solid red lines depict the overall change in predictive performance in our study population



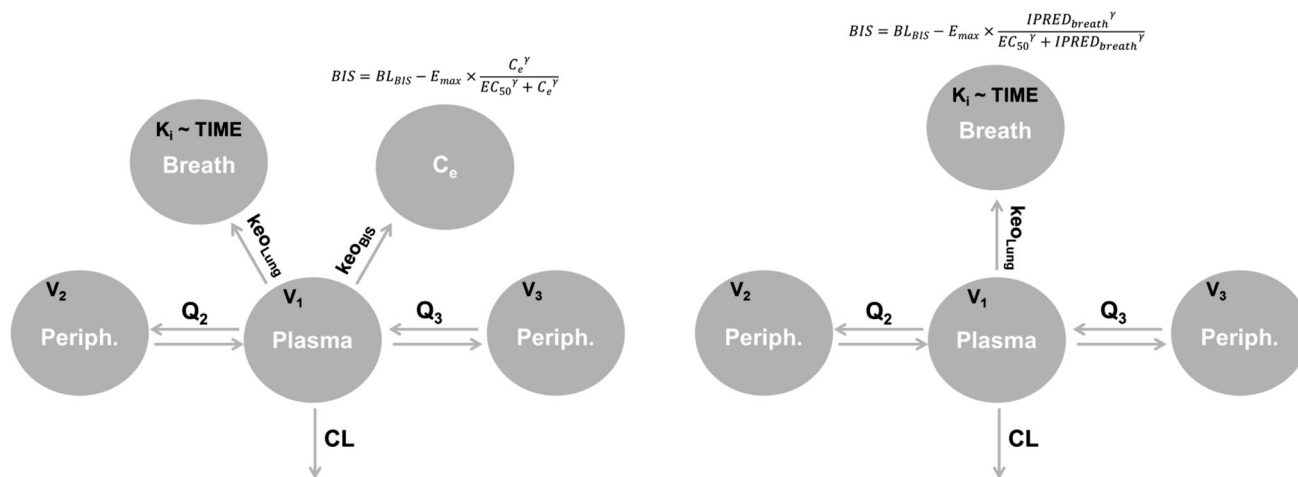


**Fig. 6** A graphical representation of both pharmacokinetic/pharmacodynamic models that were fitted to the data to describe the cerebral effects of propofol. The *left model* is the simplified version of the model proposed by Bjornsson et al. [17], whereas the *right model* is our final model with a direct relationship between  $IPRED_{breath}$  and

BIS.  $keO_{Lung}$  rate constant for the lung effect compartment,  $keO_{BIS}$  rate constant for the BIS effect compartment,  $K_i$  individual scaling parameter for the lung compartment,  $BL_{BIS}$  typical value for the BIS at baseline,  $C_e$  propofol concentration in the effect compartment,  $BIS$  bispectral index monitor

well-defined breath concentration peak, appears to be sufficiently informative to individualize the a priori model predictions. Therefore, a different clinical setting, in which this first informative phase is absent, might require a prolonged collection of breath concentrations to achieve the maximum improvement in predictive performance.

At this point, we would like to acknowledge that the current study might overestimate the potential of our proposed approach. Although we used a cross-validation approach to build our model as well as to conduct our simulation study, some of the components, such as the linear time-correction in  $K$ , might be study specific and might not extrapolate well to other studies. A thorough validation of this approach under different clinical regimens (i.e., different dosing, shorter/longer procedures) as well as in different patient populations (as opposed to the healthy volunteers in this study) should inform on the general applicability of this approach.

Finally, we wanted to validate the utility of predicted propofol breath concentrations by investigating the correlation with a measure of propofol pharmacodynamics, i.e., BIS, frequently used in the clinic. By comparing two PKPD models, one relating BIS to  $IPRED_{breath}$  and one, more classical approach where BIS is linked to a  $C_e$  (both approaches shown in Fig. 6 and in Table 2), we showed that predicted propofol breath concentrations could serve as a surrogate to the predicted effect-site concentrations, which are frequently used in the clinic to predict the cerebral effects of propofol. In this respect, the  $EC_{50}$  of 12.4 ppb might provide an alternative measurable target to the established hypothetical effect compartment  $EC_{50}$  of 2.71  $\mu\text{g/mL}$ .

## 5 Conclusions

In this work, we showed that the current state-of-the-art, propofol plasma PK model is easily extended to allow prediction of exhaled propofol concentrations. Furthermore, for the first time, we showed that monitoring of propofol breath concentrations could significantly improve the predictive performance of intraoperative propofol concentrations, thereby allowing further treatment individualization and a more stringent control on the targeted plasma concentrations during general anesthesia.

Finally, using two different versions of a PKPD model, we showed that the predicted breath concentrations are a suitable alternative to the currently used predicted effect-site concentrations to describe/predict the cerebral effects of propofol.

**Acknowledgments** None to declare.

### Compliance with Ethical Standards

**Funding** The healthy volunteer study was supported by an unrestricted research grant from V&F Medical Development GmbH, Absam, Austria.

**Conflict of interest** P Colin, D.J. Eleveld, J.P. van den Berg, H.E.M. Vereecke, M.M.R.F. Struys, G. Schelling, C.C. Apfel, and C. Hornuss have no conflicts of interest that are relevant to the content of this manuscript. None of the authors were/are involved in the commercialization of a propofol breath sensor.

## References

1. Motamed C, Devys JM, Debaene B, Billard V. Influence of real-time Bayesian forecasting of pharmacokinetic parameters on the

- precision of a rocuronium target-controlled infusion. *Eur J Clin Pharmacol.* 2012;68:1025–31.
2. Maitre PO, Stanski DR. Bayesian forecasting improves the prediction of intraoperative plasma concentrations of alfentanil. *Anesthesiology.* 1988;69:652–9.
  3. ClinicalTrials.gov. NCT01549639. Blood propofol measurement during anaesthesia using propofol target controlled infusion. Available from: <https://clinicaltrials.gov/ct2/show/NCT01549639?term=TCI+and+propofol&rank=35>. Accessed 5 Dec 2015.
  4. ClinicalTrials.gov. NCT01932424. Blood propofol concentrations in children during spinal surgery. <https://clinicaltrials.gov/ct2/show/NCT01932424?term=Sphere+medical+and+propofol&rank=1>. Accessed 5 Dec 2015.
  5. Marsh B, White M, Morton N, Kenny GN. Pharmacokinetic model driven infusion of propofol in children. *Br J Anaesth.* 1991;67:41–8.
  6. Schnider TW, Minto CF, Gambus PL, et al. The influence of method of administration and covariates on the pharmacokinetics of propofol in adult volunteers. *Anesthesiology.* 1998;88:1170–82.
  7. Eleveld DJ, Proost JH, Cortinez LI, Absalom AR, Struys MM. A general purpose pharmacokinetic model for propofol. *Anesth Analg.* 2014;118:1221–37.
  8. Katoh T, Ikeda K. The minimum alveolar concentration (MAC) of sevoflurane in humans. *Anesthesiology.* 1987;66:301–3.
  9. Lockwood G. Pharmacokinetics of inhaled anesthetics. In: Evers AS, Maze M, Kharasch ED, editors. *Anesthetic pharmacology basic principles and clinical practice*, vol. 2. New York: Cambridge Medicine; 2011. p. 385–96.
  10. Ziaian D, HR, Kleiboemer K, Hengstenberg A, Grossherr M, Brandt S, Gehring H, Zimmermann S, Berggreen A. Pharmacokinetic modeling of the transition of propofol from blood plasma to breathing gas. In: 2014 IEEE international symposium on medical measurements and applications (MeMeA), p. 1–5.
  11. Varadarajan BT. Monitoring of propofol in breath; pharmacokinetic modeling and design of a control system. Doctoral Degree Doctoral Thesis. Luebeck: Luebeck University; 2011.
  12. Grossherr M, Hengstenberg A, Dibbelt L, et al. Blood gas partition coefficient and pulmonary extraction ratio for propofol in goats and pigs. *Xenobiotica.* 2009;39:782–7.
  13. Hornuss C, Wiepcke D, Praun S, Dolch ME, Apfel CC, Schelling G. Time course of expiratory propofol after bolus injection as measured by ion molecule reaction mass spectrometry. *Anal Bioanal Chem.* 2012;403:555–61.
  14. Kreuer S, Hauschild A, Fink T, Baumbach JI, Maddula S, Volk T. Two different approaches for pharmacokinetic modeling of exhaled drug concentrations. *Sci Rep.* 2014;4:5423.
  15. Hornuss C, Dolch ME, Janitz S, et al. Determination of breath isoprene allows the identification of the expiratory fraction of the propofol breath signal during real-time propofol breath monitoring. *J Clin Monit Comput.* 2013;27:509–16.
  16. Zhang L, Beal SL, Sheiner LB. Simultaneous vs. sequential analysis for population PK/PD data I: best-case performance. *J Pharmacokinet Pharmacodyn.* 2003;30:387–404.
  17. Bjornsson MA, Norberg A, Kalman S, Karlsson MO, Simonsson US. A two-compartment effect site model describes the bispectral index after different rates of propofol infusion. *J Pharmacokinet Pharmacodyn.* 2010;37:243–55.
  18. Buil-Bruna N, Lopez-Picazo JM, Moreno-Jimenez M, Martin-Algarra S, Ribba B, Troconiz IF. A population pharmacodynamic model for lactate dehydrogenase and neuron specific enolase to predict tumor progression in small cell lung cancer patients. *AAPS J.* 2014;2014(16):609–19.
  19. Baker MT, Naguib M. Propofol: the challenges of formulation. *Anesthesiology.* 2005;103:860–76.
  20. Masui K, Kira M, Kazama T, Hagihira S, Mortier EP, Struys MM. Early phase pharmacokinetics but not pharmacodynamics are influenced by propofol infusion rate. *Anesthesiology.* 2009;111:805–17.
  21. Struys MM, Coppens MJ, De Neve N, et al. Influence of administration rate on propofol plasma-effect site equilibration. *Anesthesiology.* 2007;107:386–96.
  22. Chinery RL, Gleason AK. A compartmental model for the prediction of breath concentration and absorbed dose of chloroform after exposure while showering. *Risk Anal.* 1993;13:51–62.
  23. McKone TE. Linking a PBPK model for chloroform with measured breath concentrations in showers: implications for dermal exposure models. *J Exposure Anal Environ Epidemiol.* 1993;3:339–65.
  24. King J, Koc H, Unterkofler K, et al. Physiological modeling of isoprene dynamics in exhaled breath. *J Theor Biol.* 2010;267:626–37.
  25. King J, Unterkofler K, Teschl G, et al. A mathematical model for breath gas analysis of volatile organic compounds with special emphasis on acetone. *J Math Biol.* 2011;63:959–99.
  26. Levitt DG, Schnider TW. Human physiologically based pharmacokinetic model for propofol. *BMC Anesthesiol.* 2005;5:4.
  27. Edgington AN, Schmitt W, Willmann S. Application of physiology-based pharmacokinetic and pharmacodynamic modeling to individualized target-controlled propofol infusions. *Adv Ther.* 2006;23:143–58.
  28. Gill KL, Gertz M, Houston JB, Galetin A. Application of a physiologically based pharmacokinetic model to assess propofol hepatic and renal glucuronidation in isolation: utility of in vitro and in vivo data. *Drug Metab Dispos.* 2013;41:744–53.